ECCOMAS Congress 2016
VII European Congress on Computational Methods in Applied Sciences and Engineering
M. Papadrakakis, V. Papadopoulos, G. Stefanou, V. Plevris (eds.)
Crete Island, Greece, 5–10 June 2016

THE INLET AND OUTLET BOUNDARY PROBLEM WITH THE PREFERENCE OF MASS FLOW

Martin Kyncl, and Jaroslav Pelant

VZLÚ
Beranových 130, Prague, 19900, CZECH REPUBLIC
e-mail: kyncl@vzlu.cz, pelant@vzlu.cz

Keywords: CFD, Compressible Flow, the Navier-Stokes Equations, the Riemann Problem, Boundary Conditions, Mass Flow.

Abstract. *We work with the numerical solution of the turbulent compressible gas flow, and we focus on the numerical solution of these equations, and on the boundary conditions. In this work we focus on the inlet and outlet boundary condition with the preference of given mass flow. Usually, the boundary problem is being linearized, or roughly approximated. The inaccuracies implied by these simplifications may be small, but it has a huge impact on the solution in the whole studied area, especially for the non-stationary flow. The boundary condition with the preference of mass flow is sometimes being implemented with the use of some iterative process, guessing the correct values (for the pressure, density, velocity) in order to match the given mass flow through the boundary. In our approach we try to be as exact as possible, using our own original procedures. We follow the exact solution of the initial-value problem for the system of hyperbolic partial differential equations. This complicated problem is modified at the close vicinity of boundary, where the conservation laws are supplied with the additional boundary conditions. We complement the boundary problem suitably, and we show the analysis of the resulting uniquely-solvable modified Riemann problem. The resulting algorithm was coded and used within our own developed code for the solution of the compressible gas flow (the Euler, NS, and RANS equations). The examples show good behaviour of the analyzed boundary conditions.*

1 INTRODUCTION

The physical theory of the compressible fluid motion is based on the principles of conservation laws of mass, momentum, and energy. The mathematical equations describing these fundamental conservation laws form a system of partial differential equations. We focus on the numerical solution of these equations. We choose the well-known finite volume method to discretize the analytical problem, represented by the system of the equations in generalized (integral) form. To apply this method we split the area of the interest into the elements, and we construct a piecewise constant solution in time. The crucial problem of this method lies in the evaluation of the so-called fluxes through the edges/faces of the particular elements. We use the analysis of the exact solution of the Riemann problem for the discretization of the fluxes through the boundary edges/faces. We use own algorithms for the solution of the boundary problem, and we use it in the numerical examples.

2 THE RIEMANN PROBLEM FOR THE EULER EQUATIONS

For many numerical methods dealing with the two or three dimensional equations, describing the compressible flow, it is useful to solve the Riemann problem for the *3D split* Euler equations. We search the solution of the system of partial differential equations in time t and space (x, y, z)

$$\begin{array}{c} \frac{\partial \varrho}{\partial t} + \frac{\partial \varrho u}{\partial x} = 0 \\ \frac{\partial \varrho u}{\partial t} + \frac{\partial (p+\varrho u^2)}{\partial x} = 0 \\ \frac{\partial \varrho v}{\partial t} + \frac{\partial \varrho uv}{\partial x} = 0 \\ \frac{\partial \varrho w}{\partial t} + \frac{\partial \varrho uw}{\partial x} = 0 \\ \frac{\partial E}{\partial t} + \frac{\partial u(E+p)}{\partial x} = 0, \end{array} \tag{1}$$

equipped with the initial conditions

$$\varrho(x,t) = \varrho_L, \boldsymbol{v}(x,t) = \boldsymbol{v}_L, p(x,t) = p_L, \quad x < 0, \tag{2}$$

$$\varrho(x,t) = \varrho_R, \boldsymbol{v}(x,t) = \boldsymbol{v}_R, p(x,t) = p_R, \quad x > 0. \tag{3}$$

Vector $\boldsymbol{v} = (u, v, w)$ denotes the velocity, ϱ density, p pressure, $E = \varrho e + \varrho|\boldsymbol{v}|^2$ is the total energy, with e denoting the specific internal energy. We assume the equation of state for the calorically ideal gas

$$e = \frac{p}{\varrho(\gamma - 1)}.$$

'Split' means here that we still have 5 equations in 3D, but the dependence on y, z (space coordinates) is neglected, and we deal with the system for one space variable x. The system (1) is considered in the set $Q_\infty = (-\infty, \infty) \times (0, +\infty)$. The solution of this problem is fundamentally the same as the solution of the Riemann problem for the 1D Euler equations, see [3, page 138]. In fact, the solution for the pressure, the first component of the velocity, and the density is exactly the same as in one-dimensional case. It is a characteristic feature of the hyperbolic equations, that there is a possible raise of discontinuities in solutions, even in the case when the initial conditions are smooth, see [5, page 390]. Here the concept of the classical solution is too restrictive, and therefore we seek a weak solution of this problem. To distinguish physically admissible solutions from nonphysical ones, entropy condition must be introduced, see [5, page 396]. By the solution of the problem (1),(2),(3) we mean the *weak entropy solution* of this problem in Q_∞. The analysis to the solution of this problem can be found in many books, i.e. [3], [5], [6].

Further we are concerned with the one-dimensional Euler equations.

$$\frac{\partial \boldsymbol{q}}{\partial t} + \frac{\partial \boldsymbol{f}(\boldsymbol{q})}{\partial x} = 0, \quad \text{in } Q_\infty = (-\infty, +\infty) \times (0, +\infty) \tag{4}$$

with notation $\boldsymbol{q} = (\varrho, \varrho u, E)^{\mathrm{T}}, \quad \boldsymbol{f}(\boldsymbol{q}) = (\varrho u, \varrho u^2 + p, (E+p)u)^{\mathrm{T}}$. We assume equation of state for ideal gas holds

$$p = (\gamma - 1)(E - \varrho u^2/2) \quad \text{in } Q_\infty.$$

u denotes velocity, ϱ density, p pressure. E denotes total energy. The system is hyperbolic. The Riemann problem for hyperbolic system (4) consists in finding its *entropy weak solution* in Q_∞, which satisfies the initial condition formed by two known constant states $\boldsymbol{q}_L$, $\boldsymbol{q}_R$

$$\boldsymbol{q}(x,0) = \boldsymbol{q}_L = (\varrho_L, \varrho_L u_L, E_L)^{\mathrm{T}}, \qquad x < 0, \tag{5}$$

$$\boldsymbol{q}(x,0) = \boldsymbol{q}_R = (\varrho_R, \varrho_R u_R, E_R)^{\mathrm{T}}, \qquad x > 0. \tag{6}$$

The physical analogue to this problem is so-called *shock-tube problem*.

The general theorem on the solvability of the Riemann problem can be found in [3, page 88]. The solution $\boldsymbol{q} = \boldsymbol{q}(x,t)$ of Riemann problem (4),(5),(6) is piecewise **smooth** and its general form can be seen from figure 1, where a system of half lines is drawn. These half lines define

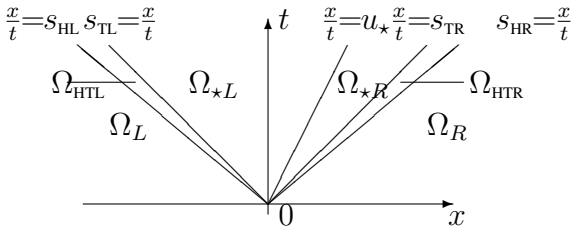

Figure 1: Structure of the solution of the Riemann problem (4),(5),(6)

regions, where $\boldsymbol{q}$ is either constant or smooth. Let us define the open sets called **wedges** (see figure 1):

$$\begin{aligned} \Omega_L &= \text{wedge}(L_{-\infty}, s_{\mathrm{HL}}), & \Omega_{\star R} &= \text{wedge}(u_\star, s_{\mathrm{TR}}), \\ \Omega_{\mathrm{HTL}} &= \text{wedge}(s_{\mathrm{HL}}, s_{\mathrm{TL}}), & \Omega_{\mathrm{HTR}} &= \text{wedge}(s_{\mathrm{TR}}, s_{\mathrm{HR}}), \\ \Omega_{\star L} &= \text{wedge}(s_{\mathrm{TL}}, u_*), & \Omega_R &= \text{wedge}(s_{\mathrm{HR}}, L_{+\infty}). \end{aligned}$$

The solution in $\Omega_L,\ \Omega_{\star L},\ \Omega_{\star R},\ \Omega_R$ is constant (see e.g. [3, page 128])

$$\begin{aligned} \boldsymbol{q}|_{\Omega_L} &= \boldsymbol{q}_L, & \boldsymbol{q}|_{\Omega_{\star R}} &= \boldsymbol{q}_{\star R}, \\ \boldsymbol{q}|_{\Omega_{\star L}} &= \boldsymbol{q}_{\star L}, & \boldsymbol{q}|_{\Omega_R} &= \boldsymbol{q}_R. \end{aligned}$$

Exact solution of the Riemann problem has three waves. The wedges Ω_L and $\Omega_{\star L}$ are separated by left wave (either 1-*shock wave*, or 1-*rarefaction wave*). There is a *contact discontinuity* in between regions $\Omega_{\star L}$ and $\Omega_{\star R}$. Wedges $\Omega_{\star R}$ and Ω_R are separated by right wave (either 3-*shock wave*, or 3-*rarefaction wave*). There are four possible wave patterns in the solution.

- ***Contact Discontinuity*** Pressure p and velocity u don't change across **contact discontinuity**, which separates $\Omega_{\star L}$ and $\Omega_{\star R}$ region in general, and moving at speed $u_\star$

$$p|_{\Omega_{\star L} \cup \Omega_{\star R}} = p_\star \ ,$$

$$u|_{\Omega_{\star L}\cup\Omega_{\star R}} = u_\star \ ,$$

In general, there is a discontinuity in density ϱ across half line $\frac{x}{t} = u_\star$

$$\varrho|_{\Omega_{\star L}} \neq \varrho|_{\Omega_{\star R}} \text{ in general.}$$

It is clear, that there must be a jump in temperature, if there is a jump in density, but not in pressure. There is also a jump in entropy. Contact discontinuity is sometimes called *entropy wave*. In reality, contact discontinuities are smeared out due to diffusive effects, which are neglected and not included in hyperbolic system (4).

It is more convenient to use the vector of primitive variables rather then the vector of conservative variables in solving the Riemann problem. Using the theory in [3], [5], [6], we can write the solution for the primitive variables as

$$\begin{aligned}
(\varrho, u, v, w, p)|_{\Omega_L} &= (\varrho_L, u_L, v_L, w_L, p_L),\\
(\varrho, u, v, w, p)|_{\Omega_{\star L}} &= (\varrho_{\star L}, u_\star, v_L, w_L, p_\star),\\
(\varrho, u, v, w, p)|_{\Omega_{\star R}} &= (\varrho_{\star R}, u_\star, v_R, w_R, p_\star),\\
(\varrho, u, v, w, p)|_{\Omega_R} &= (\varrho_R, u_R, v_R, w_R, p_R).
\end{aligned}$$

Here we show the equations for the primitive variables in $\Omega_L \cup \Omega_{HTL} \cup \Omega_{\star L}$. For the solution of the whole system see [3].

- ***1-shock wave***
  One of the possible wave patterns connecting Ω_L and $\Omega_{\star L}$ is a shock wave. Region Ω_{HTL} degenerates into single half-line. Primitive variables ϱ, u, p "jump" accross this wave. It is $u_\star < u_L, p_\star > p_L$. Inviscid shock jump relations can be derived, we call them *Rankine-Hugoniot relations*. These leads us to following relations across the 1-shock wave (see 2, or [3, page 125])

$$u_\star = u_L - (p_\star - p_L)\left(\frac{\frac{2}{(\gamma+1)\varrho_L}}{p_\star + \frac{\gamma-1}{\gamma+1}p_L}\right)^{\frac{1}{2}} \tag{7}$$

$$\varrho_{\star L} = \varrho_L \frac{\frac{\gamma-1}{\gamma+1}\frac{p_L}{p_\star} + 1}{\frac{p_L}{p_\star} + \frac{\gamma-1}{\gamma+1}} \tag{8}$$

$$s_1 = u_L - a_L\sqrt{\frac{\gamma+1}{2\gamma}\frac{p_\star}{p_L} + \frac{\gamma-1}{2\gamma}}, \tag{9}$$

  s_1 denotes speed of the 1-shock wave. Half line $\frac{x}{t} = s_1$ shapes the boundary between Ω_L and $\Omega_{\star L}$. It can be shown (see [2]), that (7) can be rewritten in the form

$$p_\star = E_{1Ls}(u_\star), \tag{10}$$

  where

$$\begin{aligned}
E_{1Ls}(u) \ = \ & p_L + \frac{\gamma+1}{4}\varrho_L(u_L-u)^2 + \\
& + \frac{(u_L-u)}{2}\sqrt{4\varrho_L\gamma p_L + \left(\frac{\gamma+1}{2}\right)^2 \varrho_L^2(u_L-u)^2},
\end{aligned} \tag{11}$$

  and $u < u_L$.

- ***1-rarefaction wave***
  Another possible left wave pattern is *rarefaction wave*. It forms Ω_{HTL} region.Variables changes smoothly within this wave. Across the 1-rarefaction wave $p_\star \leq p_L, u_\star \geq u_L$. Following equations are true.

$$u_\star = u_L + \frac{2}{\gamma - 1} a_L \left[1 - \left(\frac{p_\star}{p_L} \right)^{(\gamma-1)/2\gamma} \right] \tag{12}$$

$$\varrho_{\star L} = \varrho_L \left(\frac{p_\star}{p_L} \right)^{\frac{1}{\gamma}} \tag{13}$$

$$s_{TL} = u_\star - a_L \left(\frac{p_\star}{p_L} \right)^{(\gamma-1)/2\gamma}. \tag{14}$$

  Here $a_L = \sqrt{\gamma \frac{p_L}{\rho_L}}$ is the speed of sound in the Ω_L. s_{TL} is speed of the tail of the 1-rarefaction wave. Speed of the head of the rarefaction wave can be expressed

$$s_{HL} = u_L - a_L. \tag{15}$$

  Half line $\frac{x}{t} = s_{TL}$ shapes the boundary between Ω_L and Ω_{HTL}. Pressure positivity in (12) gives condition $u_\star < u_L + \frac{2}{\gamma-1} a_L$. Equation (12) can be written in the form

$$p_\star = p_L \left(\frac{-u_\star + u_L + \frac{2}{\gamma-1} a_L}{\frac{2}{\gamma-1} a_L} \right)^{\frac{2\gamma}{\gamma-1}}. \tag{16}$$

  State variables in Ω_{HTL} changes continuously, and can be expressed using equations (see [3], (3.1.97), page 118.)

$$\varrho(x,t) = \varrho_L \left[\frac{2}{\gamma+1} + \frac{\gamma-1}{(\gamma+1)a_L} \left(u_L - \frac{x}{t} \right) \right]^{\frac{2}{\gamma-1}}, \tag{17}$$

$$u(x,t) = \frac{2}{\gamma+1} \left[a_L + \frac{\gamma-1}{2} u_L + \frac{x}{t} \right], \tag{18}$$

$$p(x,t) = p_L \left[\frac{2}{\gamma+1} + \frac{\gamma-1}{(\gamma+1)a_L} \left(u_L - \frac{x}{t} \right) \right]^{\frac{2\gamma}{\gamma-1}}. \tag{19}$$

We combine both possibilities (10), (16) and we get *equation for pressure* $p_\star$ using values ϱ_L, u_L, p_L

$$p_\star = \begin{cases} \frac{2p_L + \frac{\gamma+1}{2}\varrho_L(u_L-u_\star)^2 + (u_L-u_\star)\sqrt{4\varrho_L\gamma p_L + \varrho_L^2(\frac{\gamma+1}{2})^2(u_L-u_\star)^2}}{2}, & u_\star < u_L \\ p_L \left(\frac{-u_\star+u_L+\frac{2}{\gamma-1}a_L}{\frac{2}{\gamma-1}a_L} \right)^{\frac{2\gamma}{\gamma-1}}, & u_L \leq u_\star < u_L + \frac{2}{\gamma-1}a_L. \end{cases} \tag{20}$$

Combining (8) and (13) we get equation for density $\varrho_{\star L}$ and pressure $p_\star$

$$\varrho_{\star L} = \begin{cases} \varrho_L \frac{\frac{\gamma-1}{\gamma+1}\frac{p_L}{p_\star}+1}{\frac{p_L}{p_\star}+\frac{\gamma-1}{\gamma+1}}, & p_\star > p_L \\ \varrho_L \left(\frac{p_\star}{p_L} \right)^{\frac{1}{\gamma}}, & p_\star \leq p_L. \end{cases} \tag{21}$$

Let us denote $s_{L?}$ the "wave speed" as follows:

$$s_{L?} = \begin{cases} s_1, & p_\star > p_L \\ s_{TL}, & p_\star \leq p_L. \end{cases}$$

In case of 1-shock wave it denotes s_1 wave speed, in the case of 1-rarefaction wave it is the speed of the tail of the wave s_{TL}. We combine (9) and (14) to obtain relation between $s_{L?}$ and $p_\star$:

$$s_{L?} = \begin{cases} u_L - a_L\sqrt{\frac{\gamma+1}{2\gamma}\frac{p_\star}{p_L} + \frac{\gamma-1}{2\gamma}}, & p_\star > p_L \\ u_\star - a_L\left(\frac{p_\star}{p_L}\right)^{(\gamma-1)/2\gamma}, & p_\star \leq p_L. \end{cases} \tag{22}$$

There are four unknowns in $\Omega_{\star L}$ to resolve in order to get the solution across left wave and the position of this wave. Relations of these unknowns $\varrho_{\star L}, p_\star, u_\star$ and the wave speed $s_{L?}$ to left state variables ϱ_L, u_L, p_L are given by three equations (20),(21),(22). To get state variables across left wave, i.e. in $\Omega_L \cup \Omega_{STL} \cup \Omega_{\star L}$, and position of the wave, we have to add another equation into the system (20),(21),(22). There is a jump in density across contact discontinuity. This brings another unknown $\varrho_{\star R}$ to unknowns $\varrho_{\star L}, p_\star, u_\star$,$s_{L?}$. We have to add two properly chosen equations into this system of equations in order to get uniquely solvable system for 5 unknowns sought in $\Omega_L \cup \Omega_{STL} \cup \Omega_{\star L} \cup \Omega_{\star R}$ region.

3 OUTLET BOUNDARY CONDITION BY THE PREFERENCE OF MASS FLOW

In this section, we attempt to solve the incomplete modified Riemann problem for the Euler equations (4),(5), seeking the solution in the general form of the Riemann problem solution, consisting of 4 constant states separated by 3 waves. Variables ϱ_L, u_L, p_L are known from the initial condition, also the speed of sound a_L is known. We add the boundary condition for the mass flow in $\Omega_{\star L}$ given as

$$u_\star \varrho_{\star L} = G_\star, \tag{23}$$

where $G_\star \geq 0$ is given constant ($G_\star = \frac{massflow}{face\ area}$). Here $u_\star$, $\varrho_{\star R}$ denotes unknown parts of the solution in the region $\Omega_{\star R}$. Velocity $u(x,t)$ and density $\varrho(x,t)$ are constant in this region, as was mentioned in 2. We are interested in the solution with $u_\star > 0$, and $s_{L?} < 0$, which guarantees the possibility of the values to be prescribed at the boundary. In general, there are two possibilities of the wave pattern, which may interest us.

- **1-shock wave**
  Here, we are interested in the solution with $s_1 < 0, u_\star > 0$. Let us construct the function $F_S(u)$, using the relations (20),(8)

$$F_S(u) = u\varrho_{\star L}(u) - G_\star, \tag{24}$$

  where

$$\varrho_{\star L}(u) = \varrho_L \frac{(\gamma-1)p_L + (\gamma+1)p(u)}{(\gamma+1)p_L + (\gamma-1)p(u)},$$

  with

$$p(u) = p_L + \frac{\gamma+1}{4}\varrho_L(u_L-u)^2 + \frac{(u_L-u)}{2}\sqrt{4\varrho_L\gamma p_L + \varrho_L^2(\frac{\gamma+1}{2})^2(u_L-u)^2}.$$

  The sought velocity $u_\star$ is the root of this function $F_S(u)$. It is $s_1 < 0$ for $u_\star < u_X = u_L\frac{2+(\gamma-1)M_L^2}{(\gamma+1)M_L^2}$, with $M_L^2 = u_L^2\varrho/\gamma p$, see [2]. The first derivative is $F_S' > 0$ for

$u < min\{u_L, u_X\}$. The iterative process can be used to compute the solution for the velocity $u_\star$ to any desired accuracy. The problem has a solution with the 1-shock wave if $F_S(min\{u_L, u_X\}) > 0$. Knowing the velocity $u_\star$, we use the relations shown above in (24) to compute the pressure $p_\star$ and the density $\varrho_{\star L}$.

Remark 1. Similarly to (24), it is possible to construct the function for the pressure. Let us use the Rankine–Hugoniot conditions across the 1-shock wave $s_1(\varrho_{\star L} - \varrho_L) + u_L\varrho_L = u_\star\varrho_{\star L}$. We construct the function with the use of (8),(9)

$$H(p) = s_1(p)\left(\varrho_{\star L}(p) - \varrho_L\right) + u_L\varrho_L - G,$$

where

$$\varrho_{\star L}(p) = \varrho_L\frac{(\gamma-1)p_L + (\gamma+1)p}{(\gamma+1)p_L + (\gamma-1)p},\ s_1(p) = u_L - a_L\sqrt{\frac{\gamma+1}{2\gamma}\frac{p}{p_L} + \frac{\gamma-1}{2\gamma}}.$$

It is $s_1'(p) < 0$, $\varrho_{\star L}'(p) > 0$ in the interval $\langle p_L, \infty)$. Further it is $(\varrho_{\star L}(p) - \varrho_L) > 0$ in this interval. We are interested in the solutions with $s_1(p) < 0$, which is satisfied for $p > p_X = p_L\left[1 + \frac{2\gamma}{\gamma+1}(M_L^2 - 1)\right]$, see [2], or analysis in [4, page 59]. The first derivative is $H'(p) = s_1'(p)\left(\varrho_{\star L}(p) - \varrho_L\right) + s_1(p)\varrho_{\star L}'(p) < 0$ in $\langle min\{p_L, p_X\}, \infty)$, and $H(min\{p_L, p_X\}) = u_L\varrho_L - G$. Now we may write

$$H(p(u)) = u\varrho_{\star L}(u) - G = F_S(u).$$

The first derivative is then $F_S'(u) = H'(p)p'(u) > 0$. Figure 2 shows the graph of the function $u\varrho_{\star L}$ for the chosen left-hand side initial conditions ϱ_L, u_L, p_L.

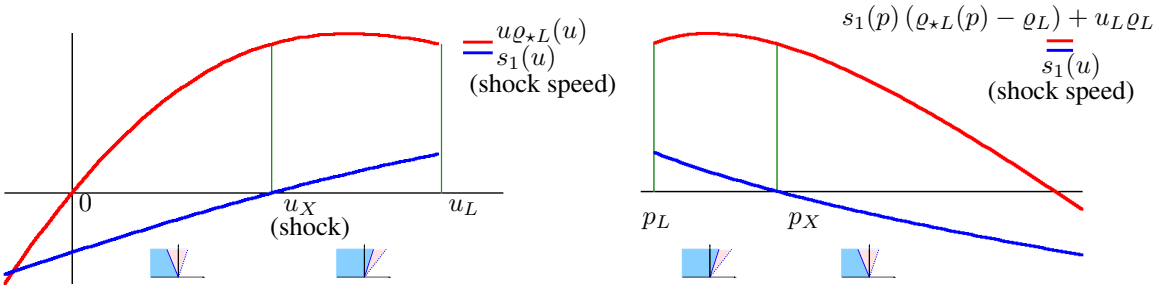

Figure 2: Example of the function $u\varrho_{\star L}(u)$ (representing the massflow in the $\Omega_{\star L}$ region), here $\gamma = 1.4, \varrho_L = 1.25, p_L = 100000, u_L = 500$. Then it is $u_X < u_L$. The function for the pressure is shown at right.

- **1-rarefaction wave**
  Let us assume the solution with the 1-rarefaction wave. From (12),(13),(23) it is

$$u_\star\varrho_L\left[1 - \frac{\gamma-1}{2a_L}(u_\star - u_L)\right]^{\frac{2}{\gamma-1}} - G_\star = 0.$$

The velocity $u_\star$ is the root of the function

$$F_R(u) = u\varrho_L\left[1 - \frac{\gamma-1}{2a_L}(u - u_L)\right]^{\frac{2}{\gamma-1}} - G_\star, \tag{25}$$

defined in the interval $u_L < u < u_L + \frac{2a_L}{\gamma-1}$. It is $F_R(u_L) = \varrho_L u_L - G_\star$. The first derivative $F_R'(u) = \varrho_L \left[1 - \frac{\gamma-1}{2a_L}(u-u_L)\right]^{\frac{2}{\gamma-1}} \left[1 - \frac{u}{a_L - \frac{\gamma-1}{2}(u-u_L)}\right]$ is zero at the points $u_1 = u_L + \frac{2a_L}{\gamma-1}$, $u_0 = \frac{\gamma-1}{\gamma+1}\left(u_L + \frac{2a_L}{\gamma-1}\right)$. Derivative $F_R'(u) > 0$ in the interval $(0, u_0)$ and $F'(u) < 0$ for $u \in (u_0, u_1)$. The maximum of the function F_R is at the point u_0. We are interested in the solution with $s_{TL} < 0$. This is satisfied only fo $u_\star < u_0$.

The problem has a solution with the 1-rarefaction wave, if $u_L < u_0$ and $F_R(u_L) \le 0$ and $F_R(u_0) \ge 0$. It is possible to compute the value $u_\star$ to any desired accuracy using the iterative method. With the velocity $u_\star$ known, we may use the relations (16), and (13). It is

$$p_\star = p_L \left[1 - \frac{\gamma-1}{2a_L}(u-u_L)\right]^{\frac{2\gamma}{\gamma-1}}, \quad \varrho_{\star L} = \varrho_L \left(\frac{p_\star}{p_L}\right)^{\frac{1}{\gamma}}.$$

Examples

Let $\gamma = 1.4, \varrho_L = 1.25, p_L = 100000$. Figures 3, 4 show the graph of the function $u\varrho_{\star L}$ for various chosen velocities u_L.

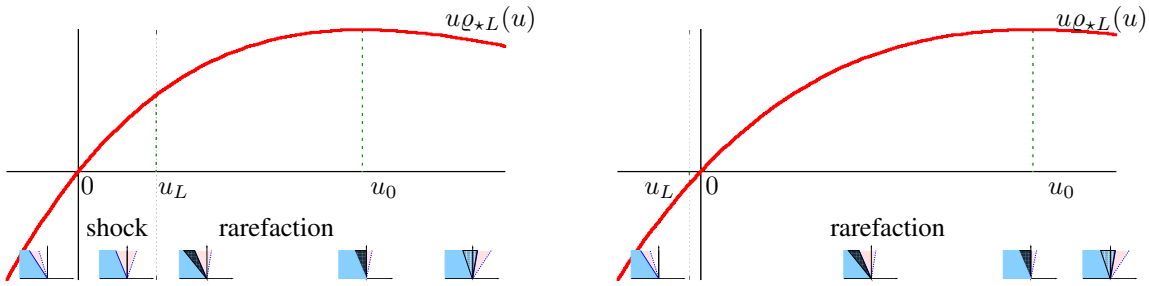

Figure 3: Examples of the function $u\varrho_{\star L}(u)$, here $u_L = 20$ (left), and $u_L = -10$ (right)..

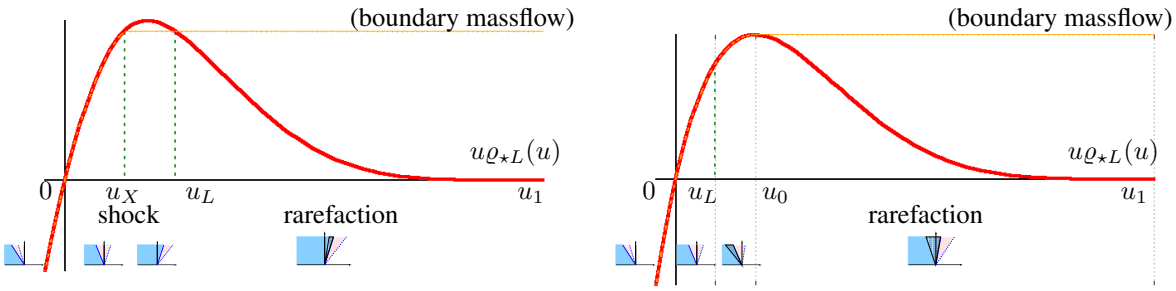

Figure 4: Examples of the function $u\varrho_{\star L}(u)$ for $u_L = 500$ (left), and $u_L = 100$ (right).

Algorithm 1D

Here we present the possible algorithm for the solution of the state values U, P, R at the boundary.

Input :

$G_\star$ . . . massflow
state inside the boundary element (as a limit to the boundary face)
ϱ_L . . . density , u_L . . . velocity , p_L . . . pressure
Output :
state values at the boundary
R . . . density , U . . . velocity , P . . . pressure

Algorithm :
if $F(u_L) > 0$ then
$U =$ root of $F_S(u),\ u \in (0, min\{u_X, u_L\}),\ (24)$. Use $(20), (8)$.
else
if $u_L > u_0$ then
$U = u_L, P = p_L, R = \varrho_L$
else
if $(u_1 < u_0)$
$U = u_1 - \varepsilon,$ use $(16), (13)$
else
if $F(u_0) < 0$ then
$U = u_0,$ use $(16), (13)$
else
$U =$ root of $F_R(u),\ u \in (u_L, u_0),\ (25)$. Use $(16), (13)$.
end
endif
end
end

Algorithm 3D

Here we present the possible algorithm for the solution of the state values at the boundary in 3D.

Input :
$G_\star$ . . . massflow
$\vec{\boldsymbol{n}}$ . . . unit outer normal to the face,
state inside the boundary element (as a limit to the boundary face)
ϱ_L . . . density
$\vec{\boldsymbol{v}} = (v_1, v_2, v_3)$ . . . velocity in global coordinate system
p_L . . . pressure
Output :
state values at the boundary
R . . . density
$\vec{\boldsymbol{V}} = (V_1, V_2, V_3)$ . . . velocity in global coordinate system
P . . . pressure

Algorithm :
1. $u_L = \vec{\boldsymbol{v}} \cdot \vec{\boldsymbol{n}} = v_1 n_1 + v_2 n_2 + v_3 n_3$
2. use **Algorithm 1D** to compute U, R, P
3. $\vec{\boldsymbol{V}} = (n_1(U - u_L) + v_1, n_2(U - u_L) + v_2, n_3(U - u_L) + v_3)$

4 INLET BOUNDARY CONDITION BY THE PREFERENCE OF MASS FLOW AND TOTAL TEMPERATURE

In this section, we analyze the incomplete modified Riemann problem for the Euler equations (4),(5), seeking the solution in the general form of the Riemann problem solution, consisting of 4 constant states separated by 3 waves. Variables ϱ_L, u_L, p_L are known from the initial condition, also the speed of sound a_L is known. We add the complementary condition for the mass flow and the total temperature in $\Omega_{\star R}$ given as

$$u_\star \varrho_{\star R} = G_\star, \tag{26}$$

$$\theta_{\star R} = \theta_0 \left(1 - \frac{\gamma - 1}{2} \frac{u_\star^2}{a_0^2}\right), \text{ with } u_\star > -\sqrt{\frac{2a_0^2}{\gamma - 1}}, \tag{27}$$

where $G_\star \leq 0$ is given constant ($G_\star = \frac{massflow}{face\ area}$). Here $u_\star,\ \varrho_{\star R}$ denotes unknown parts of the solution in the region $\Omega_{\star R}$. Further θ_0 is the prescribed total temperature, and $a_0^2 = \gamma R \theta_0$, with γ and R being gas constants. We are interested in the solution with $u_\star < 0$ (inlet boundary condition), then the computed values can be prescribed at the boundary. In general, there are two possibilities of the wave pattern, which may interest us.

Let us use the equation of state in the $\Omega_{\star R}$, giving

$$\varrho_{\star R} = \frac{p_\star}{R \theta_{\star R}}, \tag{28}$$

where $p_\star$ is the unknown pressure in the $\Omega_{\star R}$. The equation (20), introduced in section 2, can be used for this pressure. Now equation (26) can be written as

$$u_\star \frac{p_\star}{R \theta_{\star R}} = G_\star, \tag{29}$$

where $p_\star, \theta_{\star R}$ satisfy (20), (27). We seek the unknown velocity $u_\star$ as a root of the function

$$F(u) = u \frac{p(u)}{R\theta(u)} - G_\star \text{ defined for } u \in \left(-\infty, u_L + \frac{2}{\gamma - 1} a_L\right) \cap \left(-\sqrt{\frac{2a_0^2}{\gamma - 1}}, 0\right), \tag{30}$$

where

$$\theta(u) = \theta_0 \left(1 - \frac{\gamma - 1}{2} \frac{u^2}{a_0^2}\right), \quad u \in \left(-\sqrt{\frac{2a_0^2}{\gamma - 1}}, 0\right)$$

$$p(u) = \begin{cases} \frac{2p_L + \frac{\gamma+1}{2}\varrho_L (u_L - u)^2 + (u_L - u)\sqrt{4\varrho_L \gamma p_L + \varrho_L^2 (\frac{\gamma+1}{2})^2 (u_L - u)^2}}{2}, & u < u_L \\ p_L \left(\frac{-u + u_L + \frac{2}{\gamma-1} a_L}{\frac{2}{\gamma-1} a_L}\right)^{\frac{2\gamma}{\gamma-1}}, & u_L \leq u < u_L + \frac{2}{\gamma-1} a_L. \end{cases}$$

The first derivatives of these functions are $\theta'(u) = -\theta_0 \frac{\gamma-1}{2} \frac{2u}{a_o^2} > 0, p'(u) < 0$ in the its definition interval. Then it is

$$F'(u) = \frac{p(u)}{R\theta(u)} + u \frac{p'(u) R\theta(u) - p(u) R\theta'(u)}{R^2 \theta^2(u)} > 0.$$

Further it is $\lim_{u -> -\sqrt{\frac{2a_0^2}{\gamma-1}}} F(u) < 0$,and $F(min\{u_L + \frac{2}{\gamma-1} a_L, 0\}) > 0$. The function $F(u)$ is monotone, and the equation (29) has a unique solution if $u_L + \frac{2}{\gamma-1} a_L > -\sqrt{\frac{2a_0^2}{\gamma-1}}$.

Examples

Let $\theta_0 = 273.15, \gamma = 1.4, \varrho_L = 1.25, p_L = 100000$. Figures 5-8 show the graph of the function $F(u)$ and the function $u\varrho_{\star R(u)}$ for various chosen velocities u_L.

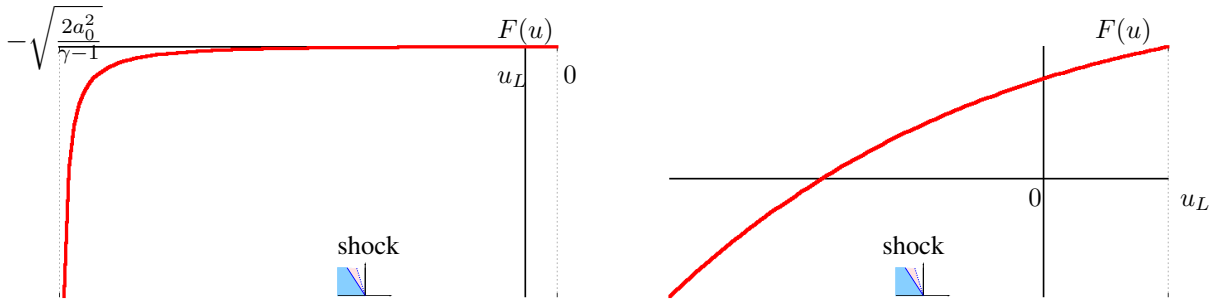

Figure 5: Graph of the function $F(u)$ for given values $\theta_0 = 273.15, \gamma = 1.4, \varrho_L = 1.25, p_L = 100000, u_L = 50, G_\star = -200$. The right picture shows detail in the restricted interval.

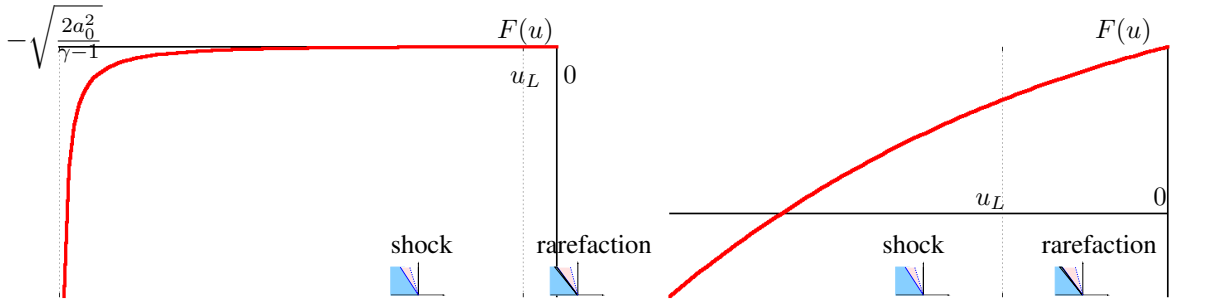

Figure 6: Graph of the function $F(u)$ for given values $\theta_0 = 273.15, \gamma = 1.4, \varrho_L = 1.25, p_L = 100000, u_L = -50, G_\star = -200$. The right picture shows detail in the restricted interval.

Remark.

The equation (26) can be written as

$$u_\star p_\star = G_\star R\theta_0 \left(1 - \frac{\gamma-1}{2}\frac{u_\star^2}{a_0^2}\right). \tag{31}$$

Now we may use (20), and seek the velocity $u_\star$ as a root of the function

$$F(u) = up(u) - G_\star R\theta_0 \left(1 - \frac{\gamma-1}{2}\frac{u^2}{a_0^2}\right),$$

with

$$p(u) = \begin{cases} \frac{2p_L + \frac{\gamma+1}{2}\varrho_L(u_L-u)^2 + (u_L-u)\sqrt{4\varrho_L\gamma p_L + \varrho_L^2(\frac{\gamma+1}{2})^2(u_L-u)^2}}{2}, & u < u_L \\ p_L\left(\frac{-u+u_L+\frac{2}{\gamma-1}a_L}{\frac{2}{\gamma-1}a_L}\right)^{\frac{2\gamma}{\gamma-1}}, & u_L \le u < u_L + \frac{2}{\gamma-1}a_L. \end{cases}$$

The first derivative is

$$F'(u) = p(u) + up'(u) + G_\star R\theta_0 \frac{\gamma-1}{2}\frac{2u}{a_0^2}.$$

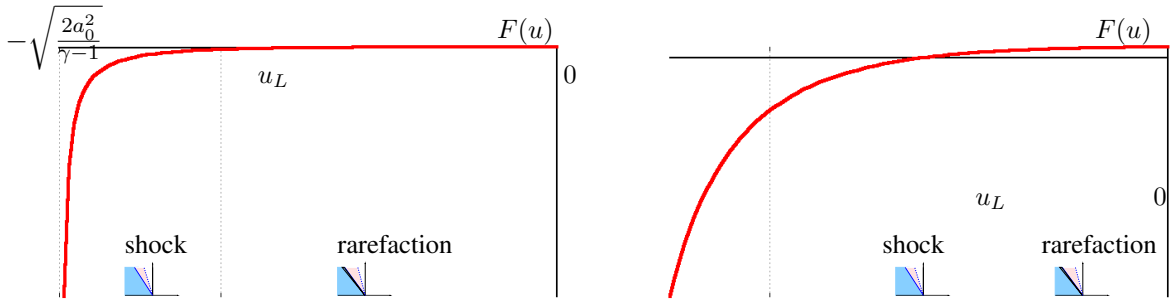

Figure 7: Graph of the function $F(u)$ for given values $\theta_0 = 273.15, \gamma = 1.4, \varrho_L = 1.25, p_L = 100000, u_L = -500, G_\star = -200$. The right picture shows detail in the restricted interval.

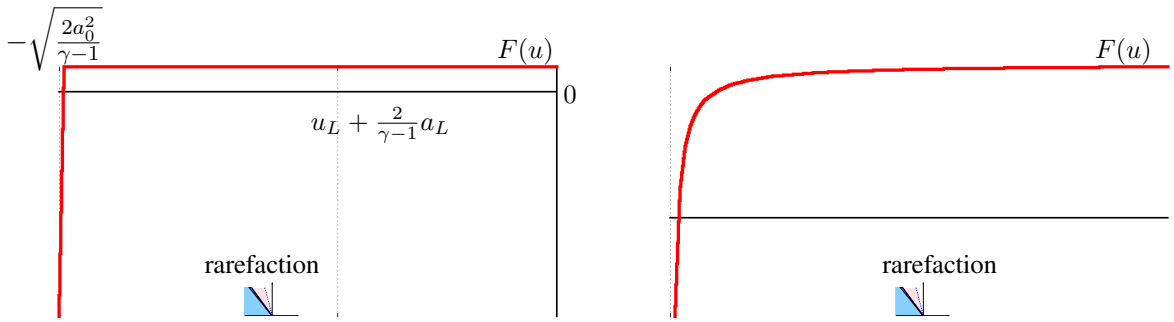

Figure 8: Graph of the function $F(u)$ for given values $\theta_0 = 273.15, \gamma = 1.4, \varrho_L = 1.25, p_L = 100000, u_L = -2000, G_\star = -200$. The right picture shows detail in the restricted interval.

It is $p(u) > 0$, $p'(u) < 0$, $u < 0$, $G_\star < 0$, and therefore it must be $F_S'(u) > 0$. Further it is $F(0) = -G_\star R\theta_0 > 0$ for $G_\star < 0$, and $F(-\sqrt{\frac{2a_0^2}{\gamma-1}}) < 0$. We seek the root of this function in the interval $u \in \left(max\{u_L, A\}, min\{0, u_L + \frac{2}{\gamma-1}a_L\}\right)$. Figures 9, 10 show the graph of the function $F(u)$ and the function $u\varrho_{\star R(u)}$ for chosen velocities u_L and input data.

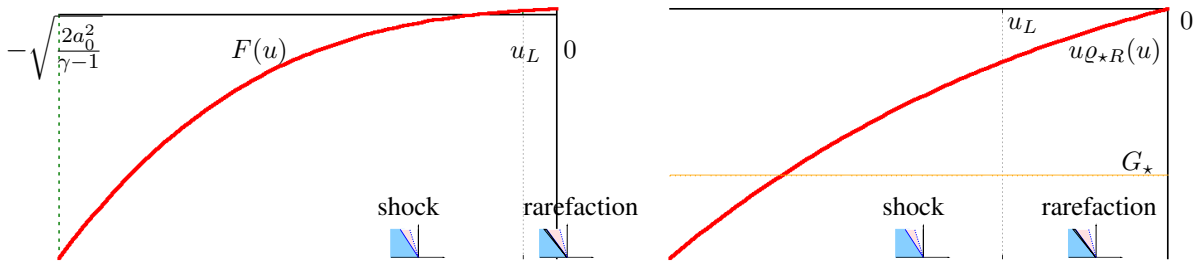

Figure 9: Graph of the function $F(u)$ (left) for given values $\theta_0 = 273.15, \gamma = 1.4, \varrho_L = 1.25, p_L = 100000, u_L = -50, G_\star = -200$. The right graph shows the massflow function $u\varrho_{\star R}(u)$.

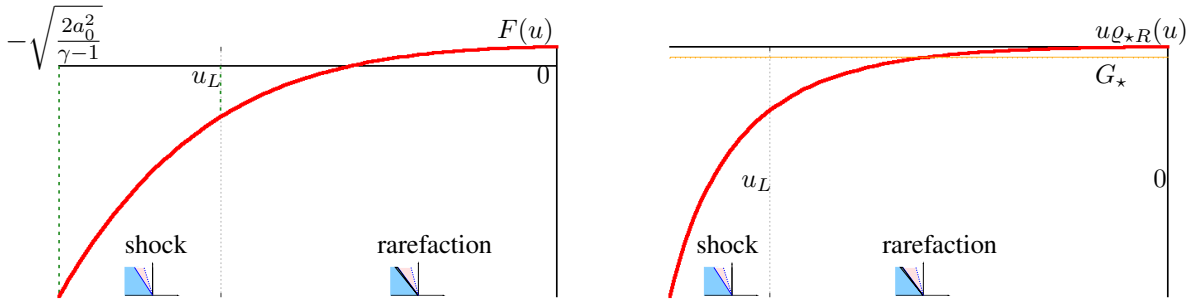

Figure 10: Graph of the function $F(u)$ (left) for given values $\theta_0 = 273.15, \gamma = 1.4, \varrho_L = 1.25, p_L = 100000, u_L = -500, G_\star = -200$. The right graph shows the massflow function $u\varrho_{\star R}(u)$.

Algorithm 1D

Here we present the algorithm for the solution of the state values U, P, R at the boundary.

Input :

$G_\star$ . . . massflow

θ_0 . . . total temperature

state inside the boundary element (as a limit to the boundary face)

ϱ_L . . . density

u_L . . . velocity

p_L . . . pressure

Output :

state values at the boundary

R . . . density , U . . . velocity , P . . . pressure

Algorithm :

1. $a_0^2 = \gamma R\theta_0,\ a_L = \sqrt{\frac{\gamma p_L}{\varrho_L}},\ A = -\sqrt{\frac{2a_0^2}{\gamma-1}}$.

if $(u_L + \frac{2}{\gamma-1}a_L < A)$ then

ERROR, NO SOLUTION. bad input data - low temperture at the inlet

else

$F(u_L) = u_L p_L - G_\star R\theta_0 \left(1 - \frac{\gamma-1}{2}\frac{u_L^2}{a_0^2}\right)$

if $(F(u_L) > 0)$ then

$U =$ root of $F_S(u) = up(u) - G_\star R\theta_0 \left(1 - \frac{\gamma-1}{2}\frac{u^2}{a_0^2}\right),\ u \in (A, u_L\rangle\,,$

$p(u) = \frac{2p_L + \frac{\gamma+1}{2}\varrho_L(u_L-u)^2 + (u_L-u)\sqrt{4\varrho_L\gamma p_L + \varrho_L^2(\frac{\gamma+1}{2})^2(u_L-u)^2}}{2}.$

else

$U =$ root of $F_R(u),\ u \in \left(max\{u_L, A\}, min\{0, u_L + \frac{2}{\gamma-1}a_L\}\right),$

$F_R(u) = up(u) - G_\star R\theta_0 \left(1 - \frac{\gamma-1}{2}\frac{u^2}{a_0^2}\right),\ p(u) = p_L\left(\frac{-u+u_L+\frac{2}{\gamma-1}a_L}{\frac{2}{\gamma-1}a_L}\right)^{\frac{2\gamma}{\gamma-1}}.$

endif

use (26), (20): $R = G_\star/u_\star,\ P = p(u_\star)$.

endif

Algorithm 3D + massflow + total temperature + tangential velocity

Here we present the possible algorithm for the solution of the state values at the boundary face in 3D.

Input:

$G_\star$ . . . massflow

$\tilde{\theta}_0$ . . . total temperature

$\vec{\boldsymbol{n}}$ . . . unit outer normal to the face, $\vec{\boldsymbol{o}}, \vec{\boldsymbol{p}}$ are tangential directions $(|\vec{\boldsymbol{o}}| = 1, \vec{\boldsymbol{p}} = \vec{\boldsymbol{n}} \times \vec{\boldsymbol{o}})$

v_t, w_t . . . tangential velocity components, v_t in the direction $\vec{\boldsymbol{o}}$, w_t in the direction $\vec{\boldsymbol{p}}$

state inside the boundary element (as a limit to the boundary face)

ϱ_L . . . density

$\vec{\boldsymbol{v}} = (v_1, v_2, v_3)$ . . . velocity in global coordinate system

p_L . . . pressure

Output:

state values at the boundary

R . . . density

$\vec{\boldsymbol{V}} = (V_1, V_2, V_3)$ . . . velocity in global coordinate system

P . . . pressure

Algorithm:

1. $\theta_0 = \tilde{\theta}_0\left(1 - \frac{\gamma-1}{2\gamma R\tilde{\theta}_0}(v_t^2 + w_t^2)\right),\ a_0^2 = \gamma R\theta_0,\ u_L = \vec{\boldsymbol{v}} \cdot \vec{\boldsymbol{n}} = v_1n_1 + v_2n_2 + v_3n_3$
2. use **Algorithm 1D** to compute U, R, P
3. $\vec{\boldsymbol{V}} = (n_1U + o_1v_t + p_1w_t, n_2U + o_2v_t + p_2w_t, n_3U + o_3v_t + p_3w_t)$

5 EXAMPLES

The developed software with presented boundary conditions was used for the simulation of the compressible turbulent flow in the 3D axis-symmetrical channel. Axis x is the axis of symmetry. At the geometry crosscut shown in figure 11., the inlet is located at the upper part of the boundary, the outlet is located left. We used the following setup in the computation:

- initial condition - constant state in the whole domain,
  $\theta^o = 288.15,\ v_1^o = 0,\ v_2^o = 0,\ v_3^o = 0,\ p^o = 101325.$
- inlet boundary condition - total quantities and velocity direction
  The boundary condition conserving the total pressure, total temperature, and zero tangential velocity, with $\theta_o = 288.15, p_o = 101325.$
- outlet boundary condition (left) - preference of the mass flow
  The boundary condition shown in Section 3, was used, with $G_\star = 4.301$ in average. At each face, the value $G_\star$ was computed (in each iteration) in order to match the average (across the whole boundary).
- walls - wall boundary condition
  The boundary condition preffering the zero normal velocity was used in the case of the inviscid flow. For the viscous flow, this condition was modified by the zero velocity at the wall, and wall temperature $\theta_{WALL} = 288.15$ was set. Further $k_{WALL} = 0$ and $\omega_{WALL} = c_\omega \frac{6\mu}{\beta \varrho y_s^2}$, $c_\omega \frac{6}{\beta} = 120$. Here by y_s we mean the distance between the face and the center of the neighbouring element.

The computational mesh in 2D crosscut consisted of 73x89 quadrilaterals.

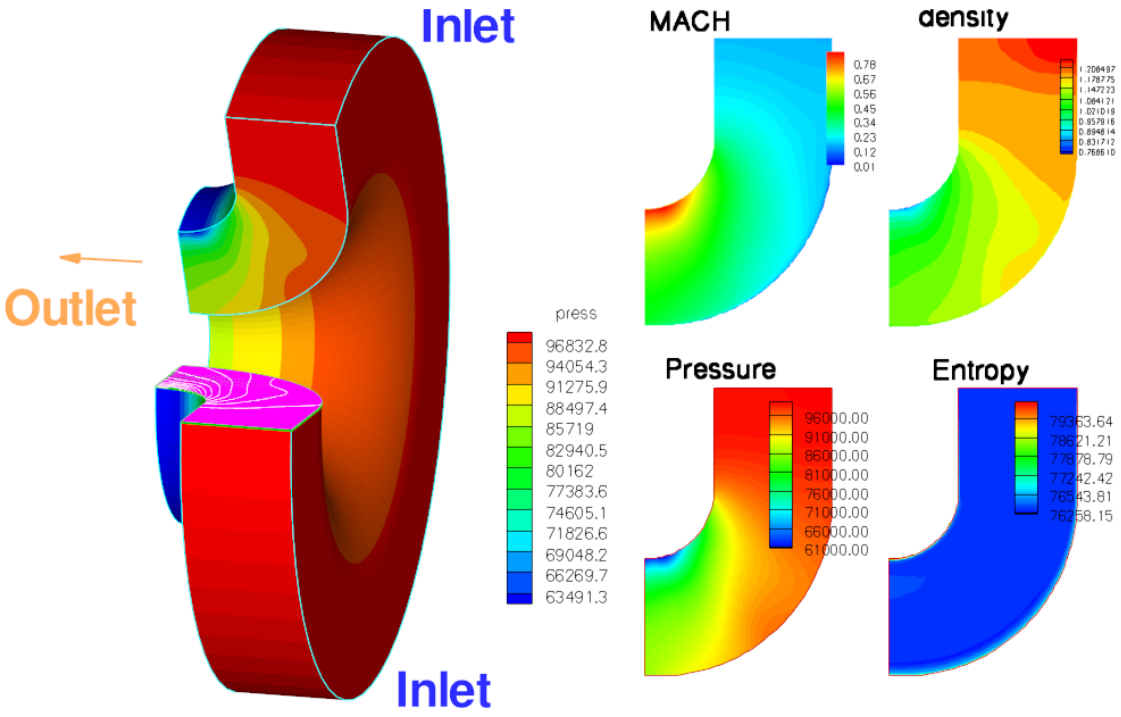

Figure 11: 3D axis-symmetrical turbulent flow, 3D geometry shape, results at chosen 2D crosscuts.

Another example with for different setup was computed, x is the axis of symmetry. At the geometry crosscut shown at figure 12., the inlet is located at the upper part of the boundary, the outlet is located left. We used the following setup for the computation:

- initial condition - constant state in the whole domain,
  $\theta^o = 273.15,\ v_1^o = 0,\ v_2^o = 0,\ v_3^o = 0,\ p^o = 101325.$
- inlet boundary condition - total quantities and velocity direction
  The boundary condition conserving the total pressure, total temperature, and zero tangential velocity, with $\theta_o = 273.15, p_o = 101325.$
- outlet boundary condition (right) - preference of the mass flow
  The boundary condition shown in Section 3, was used, with $G_\star = 4.0$ in average. At each face, the value $G_\star$ was computed (in each iteration) in order to match the average (across the whole boundary).
- walls - wall boundary condition
  The boundary condition preffering the zero normal velocity was used in the case of the inviscid flow. For the viscous flow, this condition was modified by the zero velocity at the wall, and wall temperature $\theta_{WALL} = 273.15$ was set. Further $k_{WALL} = 0$ and $\omega_{WALL} = c_\omega \frac{6\mu}{\beta \varrho y_s^2}$, $c_\omega \frac{6}{\beta} = 120$. Here by y_s we mean the distance between the face and the center of the neighbouring element.

The computational mesh in 2D crosscut consisted of 73x97 quadrilaterals.

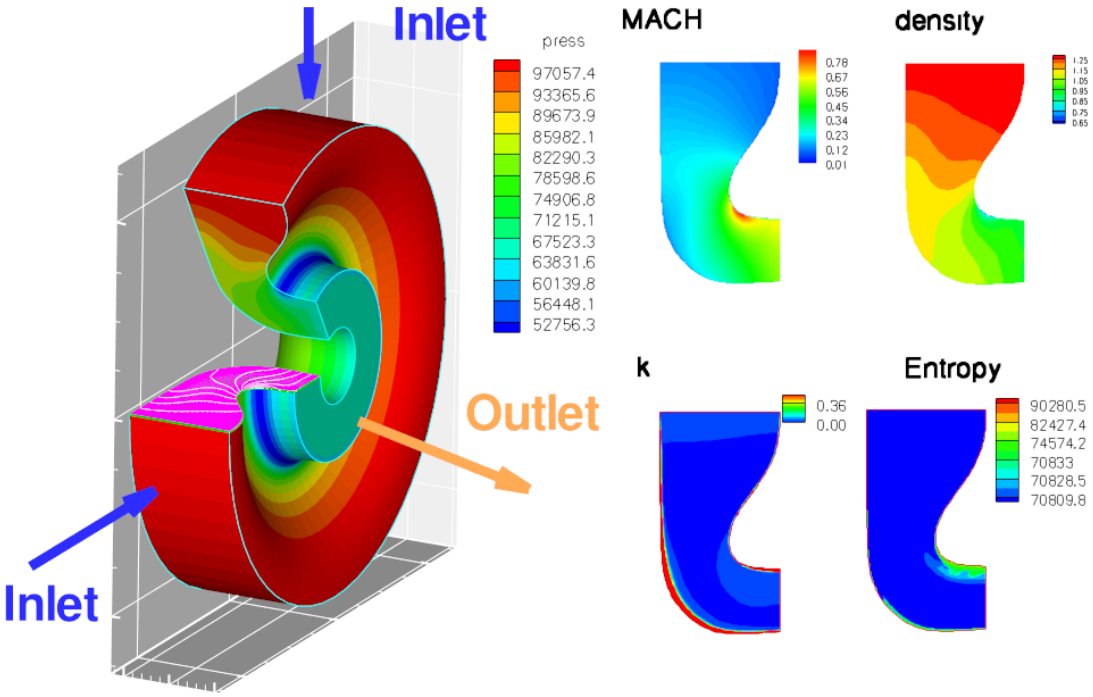

Figure 12: 3D axis-symmetrical turbulent flow, 3D geometry shape, results at chosen 2D crosscuts.

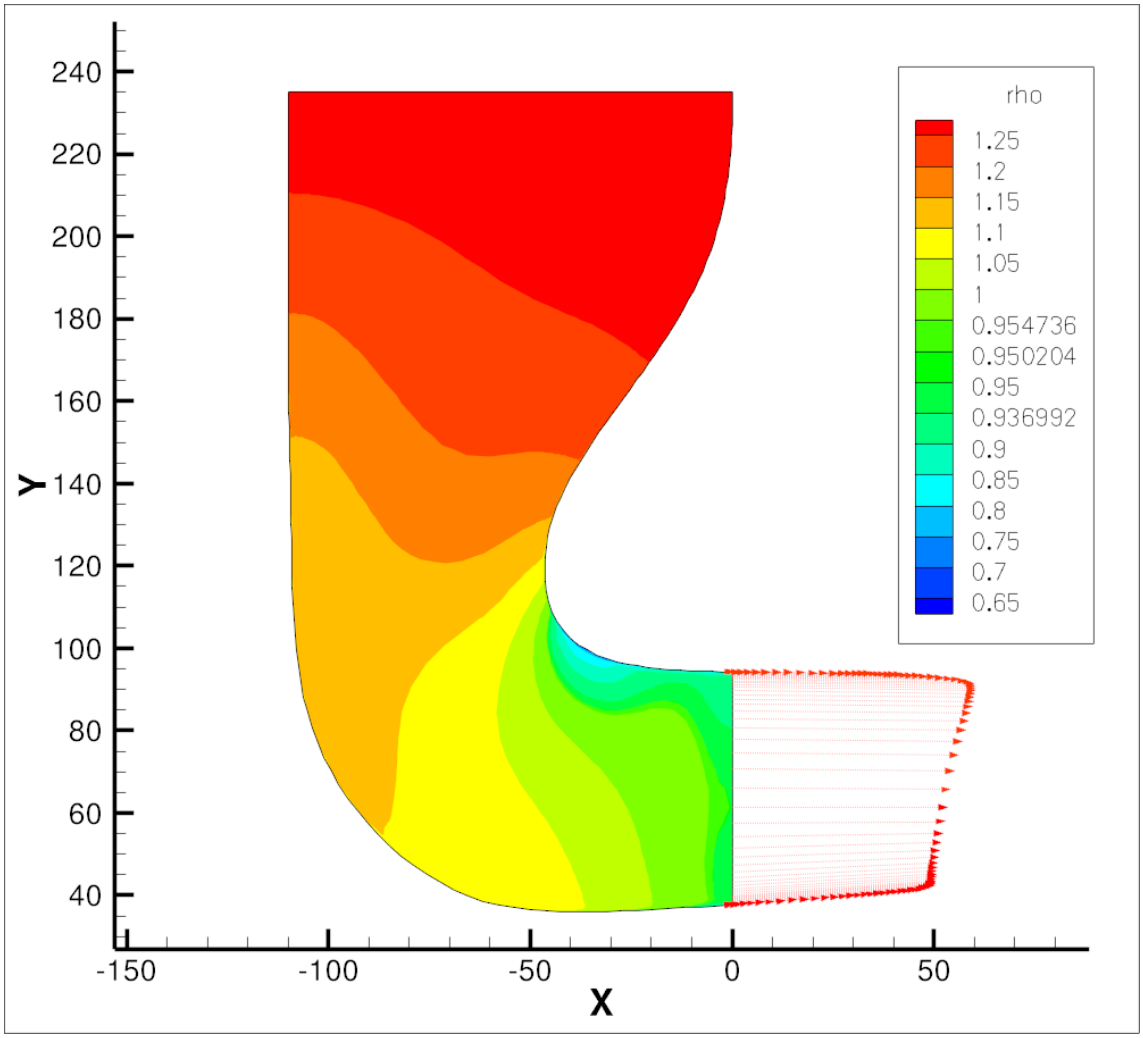

Figure 13: 3D axis-symmetrical turbulent flow, density isolines and velocity profile at the outlet, 2D crosscut.

The following example demonstrates the capabilities of the new boundary condition in the use with the unstationary gas flow. Here x is the axis of symmetry. At the geometry crosscut shown at figure 14., the inlet is located at the left part of the boundary, the outlet points away from axis x.

We used the following setup for the simulation:

- initial condition - constant state in the whole domain,
  $\theta^o = 875.00,\ v_1^o = 0,\ v_2^o = 0,\ v_3^o = 0,\ p^o = 101905.$
- inlet boundary condition - total quantities and velocity direction
  The boundary condition conserving the total pressure, total temperature, and zero tangential velocity, with $\theta_o = 875.00, p_o = 101905.$
- outlet boundary condition (right) - preference of the mass flow
  The boundary condition shown in Section 3, was used, with $G_\star = 0.75$ in average. At each face, the value $G_\star$ was computed (in each iteration) in order to match the average (across the whole boundary).
- walls - wall boundary condition
  The boundary condition preffering the zero normal velocity was used in the case of the inviscid flow. For the viscous flow, this condition was modified by the zero velocity at the wall, and wall temperature $\theta_{WALL} = 875.00$ was set. Further $k_{WALL} = 0$ and $\omega_{WALL} = c_\omega \frac{6\mu}{\beta \varrho y_s^2},\ c_\omega \frac{6}{\beta} = 120$. Here by y_s we mean the distance between the face and the center of the neighbouring element.

The computational mesh in 2D crosscut consisted of 89x87 quadrilaterals.

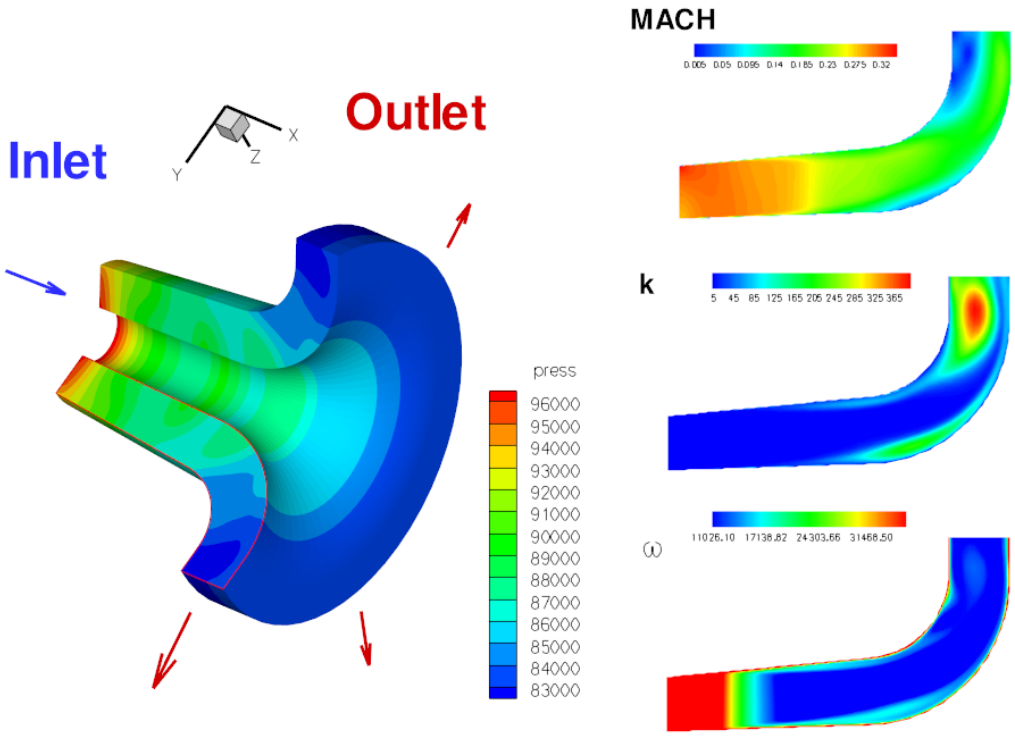

Figure 14: 3D axis-symmetrical turbulent flow, 3D geometry shape, results at chosen 2D crosscuts.

6 CONCLUSIONS

In this paper we worked with the system of equations describing the copressible gas flow in 3D. The so-called Riemann problem for the 3D split Euler equations was analyzed, together with the algorithms for the solution of the boundary problems by the preference of mass flow. The suggested algorithms were encoded into own-developed software for the solution of the compressible gas flow. Numerical examples show the use of these original boudary conditions.

Acknowledgment
This result originated with the support of Ministry of Industry and Trade of Czech Republic for the long-term strategic development of the research organisation.

REFERENCES

[1] C. J. Kok. Resolving the dependence on free-stream values for $k - \omega$ turbulence model. *AIAA Journal, Vol. 38., No. 7.*, 2000.

[2] M. Kyncl. *Numerical solution of the three-dimensional compressible flow.* Master's thesis, Prague, (2011). Doctoral Thesis.

[3] M. Feistauer, J. Felcman, and I. Straškraba. *Mathematical and Computational Methods for Compressible Flow*. Oxford University Press, Oxford, (2003).

[4] H. W. Liepmann and A. Roshko. *Elements of Gasdynamics*. John Wiley & Sons, Inc., New York, (1957).

[5] M. Feistauer. *Mathematical Methods in Fluid Dynamics*. Longman Scientific & Technical, Harlow, (1993).

[6] E. F. Toro. *Riemann Solvers and Numerical Methods for Fluid Dynamics*. Springer, Berlin, (1997).

[7] M. Kyncl and J. Pelant. Applications of the Navier-Stokes equations for 3d viscous laminar flow for symmetric inlet and outlet parts of turbine engines with the use of various boundary conditions. *Technical report R3998, VZLÚ, Beranových 130, Prague, 2006.*

[8] M. Kyncl and J. Pelant. Applications of the Navier-Stokes equations for 2d viscous, compressible turbulent flow on steady grids with the EARSM turbulent model. *Technical report R4300, VZLÚ, Beranových 130, Prague, 2007.*

[9] M. Kyncl and J. Pelant. Outlet Boundary Condition by the Preference of Mass Flow, *Technical report R6155, VZLÚ, Beranových 130, Prague, 2014.*